Accepted Manuscript

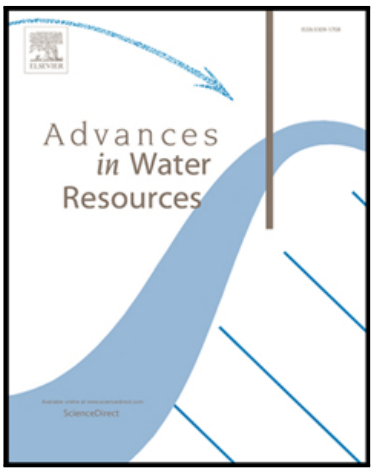

Interfacial Tension of CO_2+Brine Systems: Experiments and Predictive Modelling

Luís M.C. Pereira , Antonin Chapoy , Rod Burgass , Bahman Tohidi

PII: S0309-1708(16)30806-5
DOI: 10.1016/j.advwatres.2017.02.015
Reference: ADWR 2787

To appear in: *Advances in Water Resources*

Received date: 21 December 2016
Revised date: 24 February 2017
Accepted date: 26 February 2017

Please cite this article as: Luís M.C. Pereira , Antonin Chapoy , Rod Burgass , Bahman Tohidi , Interfacial Tension of CO_2+Brine Systems: Experiments and Predictive Modelling, *Advances in Water Resources* (2017), doi: 10.1016/j.advwatres.2017.02.015

Highlights:

- CO_2 + NaCl(aq) *IFT*s are measured from ambient conditions up to 423 K and 69.51 MPa;
- CO_2 + NaCl(aq) *IFT*s exceeded that of CO_2 + H_2O for all conditions examined;
- A predictive method, based on the DGT, is extended to CO_2 + brines;
- *IFT*s are accurately predicted for brines with ionic strength up to 2.7 $mol.kg^{-1}$;
- The developed model can predict *IFT*s relevant for CO_2 storage in saline aquifers.

Interfacial Tension of CO_2 + Brine Systems: Experiments and Predictive Modelling

Luís M.C. Pereira, Antonin Chapoy, Rod Burgass, Bahman Tohidi*

Institute of Petroleum Engineering, Heriot-Watt University, EH14 4AS Edinburgh, UK

* To whom correspondence should be addressed:

e-mail: B.Tohidi@hw.ac.uk

Phone: +44(0) 1314513672

Abstract

In this study the interfacial tension (*IFT*) between CO_2 and brines, in the context of geological storage of CO_2, was investigated. Investigations covered both experimental and theoretical aspects of this property over a broad range of conditions, including those found in subsurface formations. Measurements for CO_2 + NaCl(aq) systems, of salt molalities 0.98 and 1.98 $mol.kg^{-1}$, were performed for temperatures and pressures up to 423 K and 69.51 MPa, respectively. Results clearly showed an increase from CO_2 + H_2O *IFT* upon the addition of the salt, helping to resolve some discrepancies observed in literature data. Furthermore, a predictive method, based on the Density Gradient Theory, was extended to CO_2 + brine systems, with modelled *IFT* values yielding a good agreement with experiments from this work and literature for brines of single and mixed salts, including NaCl, KCl and $CaCl_2$, and ionic strength up to 2.7 $mol.kg^{-1}$.

Keywords: carbon dioxide, sodium chloride, interfacial tension, cubic plus association, density gradient theory.

1. Introduction

Carbon Capture and Storage (CCS) technologies are seen as one of the most promising, and technically feasible, options for significantly reducing anthropogenic CO_2 emissions [1]. Accordingly, they involve capturing CO_2 directly from large industrial sources such as coal and gas power plants, and subsequently storing it in isolated sites such as deep porous geological structures. Among possible geological sites, deep saline aquifers offer the largest CO_2 capacity, while the frequent utilization of CO_2 in enhanced oil recovery (CO_2-EOR) operations make oil and gas reservoirs more economically attractive storage options [2,3]. Though various pilot and commercial CO_2 storage projects have been successfully developed with encouraging results [4], long-term underground storage of CO_2 still presents several environmental concerns and technical challenges [5]. For example, one key issue, often of major importance for general public acceptance, concerns the safety and environmental risks of underground storage of large-scale quantities of CO_2.

One key constraint in the safe geological storage of CO_2 involves the accurate knowledge of the sealing capillary pressure which prevents the migration (*i.e.*, leakage) of CO_2 from the storage site through the caprock (structural trapping). This pressure characterises the capillary-sealing efficiency of a caprock and it corresponds to the pressure at which the non-wetting phase (CO_2) penetrates the largest pore of a caprock previously saturated with a wetting phase (typically H_2O/brine), leading to the escape of CO_2 from the storage site (reservoir). The sealing capillary pressure (or capillary entry pressure − P_{ce}) can be approximated with the Young-Laplace equation for a caprock with pores of cylindrical shape and maximum radius R as follows [3,6–8]:

$$P_{ce} = P_{CO_2} - P_{H_2O/Brine} \approx \frac{2\gamma_{CO_2-H_2O/Brine}\cos\theta}{R} \quad \textbf{(1)}$$

where θ is the contact angle of the H_2O/brine phase with the solid surface and γ is the interfacial tension between the CO_2 and the H_2O/brine phases. In this sense, the effective storage of CO_2 requires P_{ce} to be greater than the buoyancy pressure exerted by fluids in the underlying layer of the caprock; the reader is invited to read Ref. [9] for more details on this topic.

From **Eq. 1**, it becomes clear that accurate knowledge of CO_2 + H_2O/brine *IFT* over geological pressure and temperature conditions is key for the design and maximization of

CO_2 storage projects. In a previous work [10], aiming at filling in experimental gaps and resolving some discrepancies found in literature data, the *IFT* of the CO_2 + H_2O system over a broad range of pressures (up to 69 MPa) and temperatures (up to 469 K) was measured. However, the investigation of the interfacial tension between CO_2 and brine remains highly relevant as reservoir water presents dissolved ions, mostly cations such as Na^+, K^+ Ca^{2+}, Mg^{2+} and anions such as Cl^-, SO_4^- and HCO_3^-, to name just a few, and with total salt concentrations reaching or even exciding 400 $g.L^{-1}$ [11].

It is well established that the addition of salts such as NaCl, KCl, $CaCl_2$ or $MgCl_2$, affects the physical properties and phase behaviour of aqueous systems, in particular the *IFT*. Several authors [12–19] have related the increase of gas + water *IFT* upon the addition of salts to the distribution of ions between the interfacial region and the bulk aqueous phase. Johansson and Eriksson [13] reported surface tension values for different salt solutions that exceeded those of salt-free water under analogous conditions. Using the concept of an electrolyte free layer and Gibbs adsorption equation, the authors [13] showed that the *IFT* increase must be related to the negative adsorption (*i.e.*, depletion) of ions at the interface and, thereby, to their tendency to remain in the aqueous bulk phase. Hey *et al.* [20] showed that in 1:1 electrolytes solutions this increase was directly proportional to the enthalpy of hydration of ions (*i.e.*, attraction to water), suggesting that ions were preferably fully hydrated in the bulk aqueous phase than partly hydrated in the interface. In general, the attraction of cations to water molecules is stronger than anions and hence, cations are strongly repelled while anions approach more closely to the interface [13,19]. Such gradient of ions results in an electrostatic potential differential at the interface which enhances the offset of water molecules from the interface towards the aqueous bulk phase and increases the magnitude of the interfacial tension [21]. Cation hydration increases as the ratio of cation charge to cation surface area is increased and thus the impact on the *IFT* is expected to increase as follows [22]:

$$Cs^+ < Rb^+ < NH_4^+ < K^+ < Na^+ < Li^+ < Ca^{2+} < Mg^{2+} \quad \textbf{(2)}$$

The findings described above are in agreement with Molecular Dynamics simulations performed by Li *et al.* [23] for CO_2 + brine systems and salts with the chloride (Cl^-) anion over a broad range of pressure and temperature conditions. In their work, computed *IFT* values and density profiles of species across the interface also indicated a negative adsorption (negative surface excess) of ions at the interface.

Another important factor influencing the magnitude of experimentally determined *IFT* values, and often less discussed, may be associated to the density increase of the aqueous phase and gas solubility decrease ("salting-out" effect). The addition of salts increases the average molecular weight of the aqueous phase, which under the assumption that the excess volume of mixing is zero [24] results in a departure of the brine density from that of pure water. Such increase in density of the aqueous phase amplifies the density difference between phases ($\Delta\rho$). This effect greatly influences the experimental determination of *IFT* values through indirect measurement techniques which require the use of $\Delta\rho$, such as the pendant drop method. For example, at T = 373 K and P = 50 MPa, the density differences between phases of CO_2 + H_2O [10] and CO_2 + $CaCl_2$(aq) [25] systems reach a relative difference of approximately 94 and 179 % for $CaCl_2$ molalities m = 2.5 and 5.0 mol.kg^{-1}, respectively. Furthermore, in the case of gas + brine systems, the well-known salting-out effect on the gas solubility enhances the differences between the equilibrated phases promoting the increase of *IFT*.

In spite of their relevance, and somewhat surprisingly, examination of literature shows that few studies have investigated the *IFT* between CO_2 and single/binary salt solutions at reservoir conditions. These studies are limited not only in the type of salt and brine composition, as summarized in **Table 1**, but also in some cases the results are inconsistent. For example, most of these studies show that *IFT* increases with salt concentration for any temperature and pressure state. However, as can be seen in **Figure 1**, *IFT* values reported by Chalbaud *et al.* [18] and Li *et al.* [21] for different brines containing NaCl against CO_2 are lower for all salinities than those between CO_2 and pure water at T = 298 K [10,26]. It is worth nothing that Chalbaud *et al.* [18] and Li *et al.* [21] have already accounted for the increase in density of the brine-rich phase due to the dissolution of CO_2, and in turn its impact on the magnitude of the *IFT*. Therefore, it is necessary to perform further measurements to clarify such discrepancies ("low" *IFT*), especially for systems with NaCl as this is the most abundant salt in the reservoir brine [11].

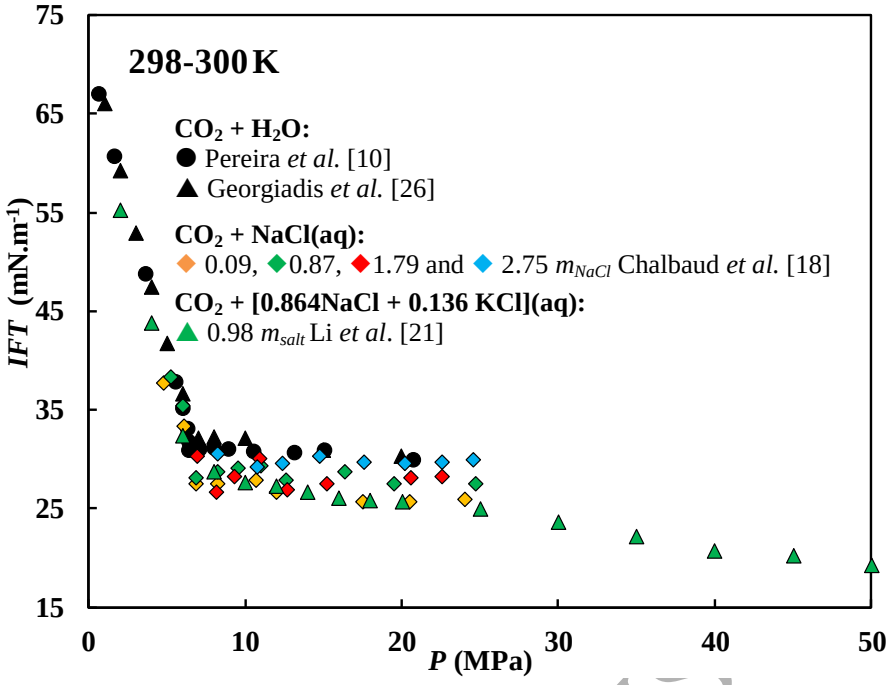

Figure 1. *IFT*-pressure diagram of CO_2 + H_2O and CO_2 + H_2O + Salt systems. *IFT* data reported by Georgiadis *et al.* [26] were recalculated considering the impact of CO_2 dissolution on the density of the aqueous phase by using a previously developed correlation [10].

Table 1. Literature *IFT* data of CO_2 + single/binary salt aqueous solutions. NA = not applicable.

***T* / K**	***P* / MPa**	**Salt 1 molality *m* (mol.kg^{-1})**	**Salt 2 molality *m* (mol.kg^{-1})**	**Source**	**Year**
NaCl (1)					
298	0.1 to 6.0	0.51 to 5.78	NA	Massoudi and King [27]	1975
308	5 to 45	0.35	NA	Chiquet *et al.* [6]	2007
300 to 373	4.8 to 25.8	0.085 to 2.75	NA	Chalbaud *et al.* [18]	2009
300 to 313	3 to 9	0.1 and 1.03	NA	Liu *et al.* [28]	2015
308 to 343	0.1 to 20	4.28	NA	Arif *et al.* [29]	2016
298 to 398	0.2 to 34.7	0.17 to 4.28	NA	Liu *et al.* [30]	2016
$CaCl_2$ (1)					
300 to 373	4.9 to 25.2	0.05 to 2.7	NA	Aggelopoulos *et al.* [31]	2010
343 to 423	2 to 50	2.5 and 5.0	NA	Li *et al.* [25]	2012
$MgCl_2$(1)					
343 to 423	2.0 to 50.0	2.5, 5.0	NA	Li *et al.* [25]	2012
Na_2SO_4 (1)					
343 to 373	2 to 16	0.49 and 0.98	NA	Li *et al.* [25]	2012
NaCl (1) + $CaCl_2$ (2)					
300 to 373	5.0 to 25.3	0.05 to 1.5	0.05 to 1.5	Aggelopoulos *et al.* [32]	2011
NaCl (1) + KaCl (2)					
298 to 448	2.0 to 50.0	0.85 to 4.28	0.13 to 0.67	Li *et al.* [21]	2012

The development of robust thermodynamic modelling tools capable of predicting the *IFT* between CO_2 and brines over geological conditions would help overcoming the difficulties associated with the experimental determination of this property as well as the costs, as such measurements require high-pressure and corrosion-resistant equipment. Additionally,

modelling tools are essential for a proper design and overall optimisation of CO_2 sequestration projects. Therefore, in this work we further explore and validate the modelling treatment proposed in a previous work [33] for predicting the *IFT* of CO_2 + brine systems. In this modelling approach, the impact of water salinity on the interfacial tension of gas + brine is accounted for by considering the impact of salts on the phase equilibria of the system, namely the salting-out effect on the solubility of gases, and the *IFT* predicted using the profile density distribution through the interface calculated within the framework of the Density Gradient Theory [34] for the corresponding hypothetical salt-free system. Such approximated treatment of effect of salts does not account for their impact on the interfacial structure. Nonetheless, as it will be shown, not only modelled CO_2 + brine *IFT*s show a linear relationship between brine molality and *IFT* increase, consistent with experimental observations, but the method can also effectively predict the additive effect of salts.

In summary, the aim of this work is to contribute with experimental *IFT* data of CO_2 + NaCl(aq) systems at conditions representative of those found in underground formations and to examine the capability of our proposed modelling approach for predicting the interfacial tension of CO_2 + brine systems by comparison with experimental data from this work and gathered from literature.

2. Experimental

2.1. Chemicals

The specification and sources of the chemicals used in this work are summarized in **Table 2**. The water used has better specifications than double-distilled water (electrical conductivity <0.02 μS.cm^{-1} at T = 298 K). Toluene and *n*-heptane were used in this work for cleaning purposes only.

Two NaCl aqueous solutions of molalities 0.98 and 1.98 mol.kg^{-1} were prepared gravimetrically by adding the salt (dried in an oven at T = 373 K for 24h) to water. The mass of salt was determined using a Mettler Toledo balance (model PB3002) with a resolution of 0.001 g and thus, the relative uncertainty in the molality of the NaCl aqueous solutions is taken equal to the purity of the salt (0.5 %).

Table 2. Suppliers and specification as stated by the supplier of the materials used in this work.

Chemical name	Supplier	Mass fraction purity	Chemical analysis
Carbon dioxide	BOC	0.99995	
Toluene	Fischer Scientific	>0.995	
n-Heptane	RathBurn Chemicals	>0.99	
Sodium Chloride	Fischer Scientific	>0.995	
Water	Sigma-Aldrich		≤0.01 ppm silicate ≤0.4 ppm Cl^- ≤0.4 ppm NO_3^- ≤1.0 ppm PO_4^{3-} ≤1.0 ppm SO_4^{2-} ≤0.01 ppm heavy metals (as Pb)

2.2. Apparatus

The high pressure/high temperature apparatus used in this work is the same used by us in a previous work [10] to measure *IFT* of the CO_2 + H_2O system; the reader is referred to this work for a detailed description of the apparatus. In summary, the *IFT* setup consists of a see-trough windowed equilibrium cell of cylindrical shape (internal volume of 23 cm^3), made of Hastelloy C-276 and with 4 fluid ports, an imaging capturing and analysing system, sample piston vessels and a hand pump.

The equilibrium cell has a capillary tube (o.d. 1.610 ± 0.001 mm) inserted through the top fluids port and positioned so a pendant drop of the brine solution can be formed at the tip of

the capillary and maintained in equilibrium with a CO_2 atmosphere. According to the applied measurement technique, the *IFT* from pendant drops was evaluated using the Axisymmetric Drop Shape Analysis (ADSA) method, commercially available through SCA 20 (Data Physics, Germany). A detailed description of the theoretical background of this method can be found elsewhere [35–38]. In short, the principle of the ADSA method is based on matching the experimental drop profile from a digitalized image to a series of Laplacian curves with known interfacial tension values. The objective function to minimise is equal to the sum of squares between the coordinates extracted through edge detection of an image of the pendant drop (experimental curve) and theoretical curves. The best calculated curve identifies the interfacial tension value (γ) which, in turn, is related to the parameters of the pendant drop by:

$$\gamma = \frac{\Delta\rho g}{(Bk_{apex})^2} \quad \textbf{(3)}$$

where $\Delta\rho$ is the density difference between the equilibrated phases, g is the gravitational acceleration and B and k_{apex} are parameters adjusted to the profile of the drop. As part of the inputs in **Eq. 3**, the density of the equilibrated phases, in the form of $\Delta\rho$, is required for an accurate estimation of the *IFT* values.

Considering the effect of CO_2 solubility on the phase density difference of the CO_2 + H_2O system and, in turn, the impact on the experimental determination of *IFT* values [6,10], it becomes also important to properly account for the effect of CO_2 dissolution on the density of NaCl solutions. Experimental CO_2-saturated liquid density data of NaCl brines were reported by Yan *et al.* [39]. In their work, the densities of CO_2-saturated solutions with NaCl molalities of 1 and 5 mol.kg^{-1} were measured using a vibrating U-tube densitometer at temperatures in the range 323 to 413 K and pressures up to 40 MPa. In order to estimate the density of the CO_2-saturated brine phase at pertinent pressure and temperature conditions, and salt molalities, the model developed by Duan *et al.* [40] was used (through computer programs mentioned therein). Accordingly, this model is a multi-parameter correlation based on the Duan *et al.* [41] EoS, and improved versions of the model [42,43], and on the theory of Pitzer [44]. The Duan model is expected to be capable of predicting the CO_2-saturated brine density of CO_2 + NaCl(aq) systems for temperatures and pressures up to 573 K and 100 MPa, respectively, and NaCl molalities up to 4.5 mol. kg^{-1}. To check the validity of this approach, deviations of the Duan *et al.* [40] model to CO_2-saturared water and CO_2-saturared brine

density data measured by Pereira *et al.* [10] and Yan *et al.* [39], respectively, were calculated and the results plotted in **Figure 2**. As can be seen, the model allows a reproduction of the density of the aqueous phase of the CO_2 + H_2O and CO_2 + NaCl(aq) systems above 99.50 % and 99.75 %, respectively, with an average absolute deviation to experimental data of 1.3 (0.13 %) and 0.7 $kg.m^{-3}$ (0.06 %), respectively, confirming to some extent the validity of this approach. In contrasts, several studies (see Refs. [6,10,45,46] and additional references mentioned therein) have shown that the departure of the density for the water-saturated CO_2 phase in the CO_2 + H_2O system from that of pure CO_2 is nearly negligible, and thus the density of this phase can be fairly approximate to that of pure CO_2 without any significant loss of accuracy in the *IFT* measurements for the range of conditions of interest. Therefore, in this work the density of water-saturated CO_2 phase was taken to be equal to that of pure CO_2, calculated using Span and Wagner EoS, as implemented in REFPROP [47], under analogous pressure and temperature conditions.

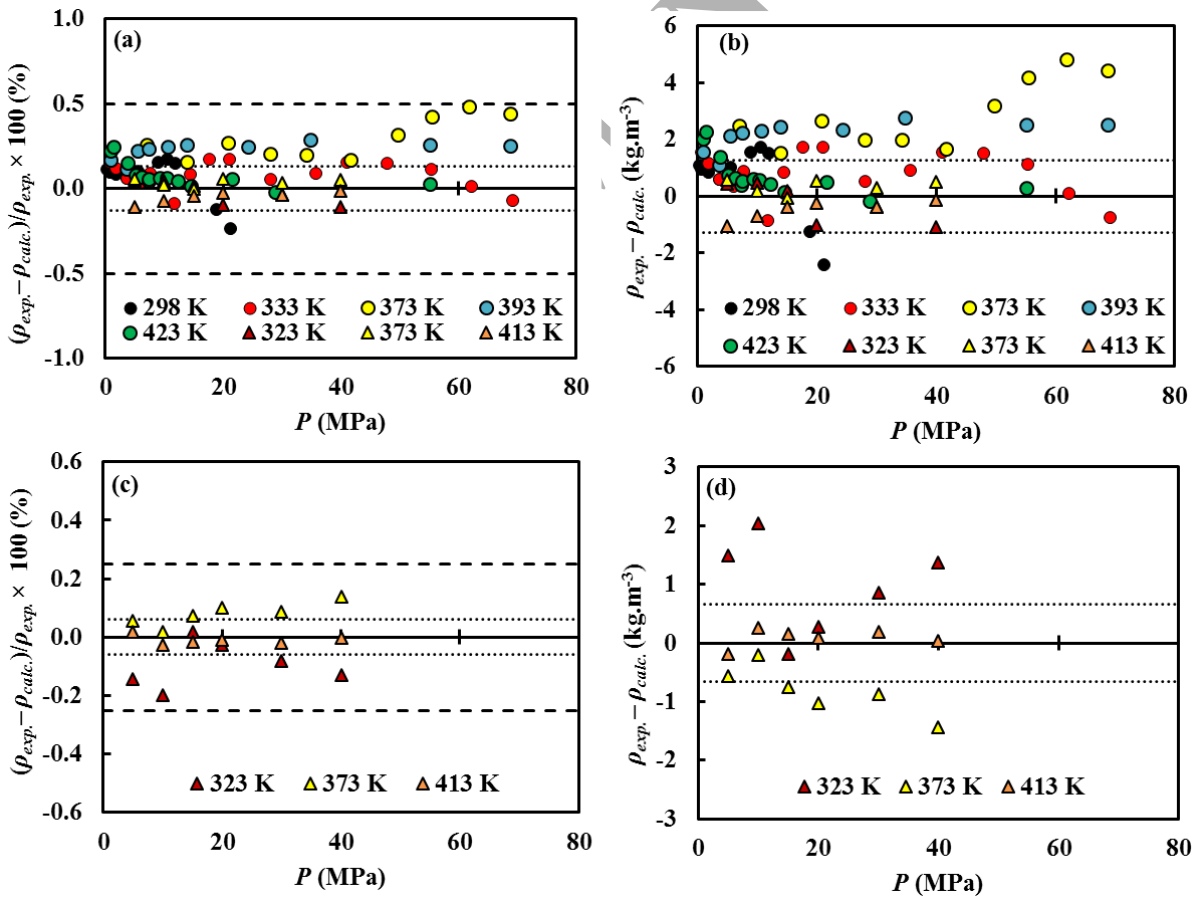

Figure 2. Relative deviation−pressure and absolute deviation−pressure diagrams of **(a** and **b)** CO_2 + H_2O and **(c** and **d)** CO_2 + NaCl(aq) (m_{NaCl} = 1 mol.kg^{-1}) systems. Symbols represent deviations of CO_2-saturated liquid

densities calculated using the Duan *et al*. [40] model to measured data from: Pereira *et al.* [10] (circles) and Yan *et al.* [39] (triangles).

2.3. Experimental Procedure

After thorough cleaning with *n*-heptane and toluene, and vacuuming of the cell, CO_2 was introduced under pressure into the cell, from a piston vessel and by means of high pressure tubing, and the pressure inside the cell maintained by isolating the cell from the CO_2 source. The tested brine was degassed by means of an ultra-sonic bath during 30 min before it was transferred to the hand pump and connected to the top of the cell. Following this, sufficient brine solution was introduced into the cell until this phase was visible on the bottom of the cell and the system left to reach equilibrium. This procedure helped ensuring saturation of the CO_2 atmosphere in water molecules. In order to measure CO_2 + NaCl(aq) *IFT* values, a drop of the brine solution was formed inside the cell at the tip of the capillary tube by means of turning the hand pump and the drop was recorded for at least 900 s and frames taken each 10 s. A minimum of 3 consecutive drops were considered for each pressure and temperature state and the *IFT* taken as the average of *IFT* values computed from frames captured within the 300^{th} and 600^{th} second.

3. Modelling

3.1. Theoretical Background

The Density Gradient Theory (DGT) is a rigorous theoretical approach which converts the statistical mechanics of inhomogeneous fluids (interface) into a set of non-linear equations to compute the density profiles ($d\rho i/dz$) of species *i* and interfacial tension values. Based on the original work of van der Waals for inhomogeneous fluids [48], and later reformulated by Cahn and Hilliard [34], the DGT is built around the minimization of the Helmholtz free energy of inhomogeneous fluid (*F*). For a planar interface of area *A* and in the absence of external forces it is given by [49]:

$$F = A\int_{-\infty}^{+\infty}\left[f_0(\rho(z)) + \sum_i\sum_j c_{ij}\frac{d\rho_i}{dz}\frac{d\rho_j}{dz}\right]dz \qquad \textbf{(4)}$$

It is clear from previous equation that the minimization of *F* involves a contribution of the Helmholtz free energy density of the homogeneous fluid (f_0) at local density $\rho(z)$ and a corrective term a corrective term consisting on the influence parameter (c_{ij}) and the density

gradients in the inhomogeneous fluid ($d\rho_i/dz$ and $d\rho_j/dz$). The density gradients in the interfacial region are calculated by solving the Euler-Lagrange equations obtained by applying the free energy minimum criterion to **Eq. 4**, which under the assumption that the influence parameters are weakly dependant on the density gradients [50,51], yields:

$$\sum_j c_{ij} \frac{d^2\rho_j}{dz^2} = \mu_i(\rho_1(z),...,\rho_N(z)) - \mu_i^{Eq.} \quad \text{for } i,j = 1\ldots N_{comp} \tag{5}$$

where μ_i are the pure component chemical potentials evaluated at each spatial point (*i.e.*, z^{th}) and at the phase equilibrium conditions of the bulk phases ($\mu_i^{Eq.}$). **Eq.5** represents the set of equations governing the density distribution of components across the interfacial region. The applied method for solving these equations is based on *i)* a discretization of the density derivatives in space *z* by a finite difference method and *ii)* solving the resultant set of non-linear equations by a Newton-Raphson iteration scheme for increasing values of interface thickness [49,52,53]. The boundary conditions of the differential problem are defined by the homogeneous phases in contact *I* and *II*: $\rho_i(z \rightarrow z^k) = \rho_i^k$ with $k = I$ and *II*. Once the density distribution across the interface is known, the *IFT* is computed by [54,55]:

$$\gamma = \int_{-\infty}^{+\infty} \left[\sum_i \sum_j c_{ij} \frac{d\rho_i}{dz} \frac{d\rho_j}{dz} \right] dz \tag{6}$$

The cross influence parameters c_{ij} are related to pure component influence parameters c_i and c_j by the following mixing rule [51]:

$$c_{ij} = (1-\beta_{ij})\sqrt{c_i c_j} \tag{7}$$

where β_{ij} is the adjustable binary interaction coefficient of influence parameters. The influence parameters relate the response of the density gradients to the local deviations of the chemical potentials from their bulk values and, in turn, the energy of the interface [49,55,56].

From what was presented above, the only inputs of the DGT are the Helmholtz free energy density of the homogeneous fluid and the influence parameters of pure components. The Helmholtz free energy density of the homogeneous fluid is accessible through an equation of state (EoS), whereas influence parameters are in general calculated from surface tension data of pure fluids or estimated from correlations available in literature (see Ref. [57] and references mentioned therein).

3.2. Modelling the CO_2 + H_2O system

Several authors [58–63] have described the *IFT* of the CO_2 + H_2O system by coupling the DGT with SAFT (Statistical Association Fluid Theory)-type EoSs. Of these, Chow *et al*. [64] applied the SAFT-VR Mie and described the *IFT* of this system over a broad range of temperatures (up to 448 K) and pressures (up to 60 MPa), with an overall deviation between calculated and experimental values of only 4.8 %. In their work, the authors used the geometric-mean of influence parameters (*i.e.*, β_{ij} = 0 in **Eq. 7**) and adopted the influence parameters to be linear functions of temperature estimated for H_2O from pure component surface tension data and for CO_2 from experimental interfacial tension data of the binary. This procedure corresponds to an attempt by the authors of overcoming the challenges that arise from the use of an influence parameter for CO_2 estimated from properties in subcritical conditions (T_c ~ 304.1 K) which, in turn, may not be enough for providing an accurate representation of the influence parameters at/or above supercritical conditions. Their method seemed to also capture effectively the *IFT* between water and sparingly soluble gases such as nitrogen (T_c ~ 126.2 K) and argon (T_c ~ 150.7 K), as well as the *IFT* of CO_2 + N_2 + H_2O and CO_2 + Ar + H_2O mixtures, with overall deviations between calculated and experimentally determined *IFT* values ranging from 1.5 to 7.9 % [64]. Other authors, such as Li *et al.* [60], Niño-Amezquita *et al.* [59] and Lafitte *et al.* [58], applied the PC-SAFT, PCP-SAFT and SAFT-VR Mie EoSs, respectively, together with constant influence parameters estimated from pure component surface tension data, and successfully modelled CO_2 + H_2O *IFT* for moderate pressures (up to 20 MPa) and temperatures (up to 344 K). Both Niño-Amezquita *et al.* [59] and Laffite *et al.* [58] used a single, temperature independent, binary coefficient different from zero in the mixing rule of influence parameters for describing correctly the *IFT* of the CO_2 + H_2O system, whereas Li *et al.* [60] opted for using the geometric-mean mixing rule and on adjusting the binary coefficients of the selected EoS (*i.e.*, k_{ij}s) simultaneously to bulk phase densities and interfacial tensions of the investigated binary system.

In our previous work [10], the DGT was combined with the Cubic-Plus-Association (CPA) EoS [65,66], and by using the geometric-mean of influence parameters along with the method proposed by Khosharay *et al.* [62,63] for estimating the influence parameters of CO_2 and H_2O, the *IFT* of the CO_2 + H_2O system was predicted over a broad range of temperatures (up to 469 K) and pressures (up to 69 MPa) with remarkably low overall deviations (4.5 %) to experimentally determined *IFT* values. The method proposed by Khosharay and co-workers

[62,63] involved correlating the influence parameters adjusted from surface tension data to saturated vapour and liquid density of pure fluids. Subsequently, the influence parameters in the mixture were estimated taking into account the molar density of each component in the bulk phases. Khosharay *et al.* applied the CK-SAFT [62] and the sPC-SAFT [63] EoSs to model the *IFT* of several aqueous binary systems including carbon dioxide, hydrogen sulphide, methane, ethane and propane, with binary interaction coefficients of the selected EoS (k_{ij}s) regressed simultaneously against density and *IFT* binary data. The method of Kosharay *et al.* [62,63] for the influence parameters seemed to improve the description of CO_2 + H_2O *IFT* when compared to using constant influence parameters calculated from surface tension data. However, their approach for the influence parameters showed negligible improvement in the modelling of the *IFT* of water against methane and ethane [62], and in the case of H_2S + H_2O *IFT*, overall deviations from experimental values from two experimental data sets were even seen to increase from 5.8 % (constant influence parameters) to 11.5 % (density dependent influence parameters) [63]. Furthermore, Khosharay and Varaminian [62] reported not being able to determine the density profiles and accompanied *IFT* of the C_3H_8 + H_2O system when using the new proposed approach for the influence parameters. Indeed, we experienced similar problems when using their influence parameter method for modelling CH_4 + H_2O *IFT* [33]. It is believed that such problems are intrinsically associated to the magnitude of the influence parameters together with the use of the geometric-mean mixing rule for the influence parameters in aqueous systems which, in turn, can lead to the appearance of infinitely steep density profiles for the adsorbed components creating numerical difficulties in the calculation of the density gradients; these results have been described in detail elsewhere [52,53].

To circumvent the constraint described above, and as a way of keeping the model accessible to a wider class of systems and the number of adjustable parameters to a minimum, it was decided to use in this work only constant influence parameters. The H_2O influence parameter was calculated using the correlation developed by Queimada *et al*. [67], whereas the CO_2 influence parameter was estimated from surface tension data [47]. H_2O and CO_2 influence parameters, calculated at fixed reduced temperatures of 0.45 and 0.72, respectively, are listed in **Table 3**. Aiming at mitigating the numerical difficulties associated to the appearance of very sharp peaks in the density profiles and at providing a correct description of CO_2 + H_2O *IFT*, a single, temperature independent, value for $\beta_{ij} \neq 0$ was used. In order to keep the modelling approach as predictive as possible, the value of β_{ij} was estimated with the aid of

one experimental binary *IFT* data point [10], at intermediate conditions (T = 374.0 K and P = 12.09 MPa), and then used to compute, in a predictive manner, tensions at other pressure and temperature conditions. The estimated value was found to amount β_{ij} = 0.27.

The required phase equilibrium properties and Helmholtz free energy density of the system were evaluated using the CPA EoS. A brief description of this EoS, along with the association scheme considered for CO_2 and H_2O and the expression used for estimating the EoS binary interaction coefficients (k_{ij}s), both established in previous works, are provided in the Supporting Information; H_2O and CO_2 CPA parameters used are listed in **Table 3**. At this point it is important to mention that the selected modelling approach ensures that both phase equilibrium properties and *IFT* values of the CO_2 + H_2O system are effectively described.

Table 3. CPA parameters and DGT influence parameters used in this work. CPA parameters for H_2O and CO_2 were taken from the works of Kontogeorgis *et al*. [68] and Tsivintzelis *et al.* [69], respectively.

	a_0 (J.m^3.mol^{-2})	c_1	b (10^{-5} m^3.mol^{-1})	ε (J.mol^{-1})	β_{CPA}	c_i (10^{-20} J m^5 mol^{-2})
H_2O	0.12277	0.6736	1.45	16655	0.0692	1.80137
CO_2	0.35079	0.7602	2.72			2.84620

Figure 3 shows a comparison between computed and experimental [10] *IFT* values of the CO_2 + H_2O system. While very good agreement was obtained at moderate and high temperatures, greater deviations were observed at low temperatures (T = 298 and 313 K), resulting in an overall percentage average absolute deviation between computed and experimental *IFT*s of 6.5 %. Nonetheless, considering the wide range of conditions examined, the results are very satisfactory. The adopted approach presents a slightly higher overall deviation than that obtained when using bulk density dependent functions for the influence parameters (4.5 %) [10], but with the advantage of being numerically stable.

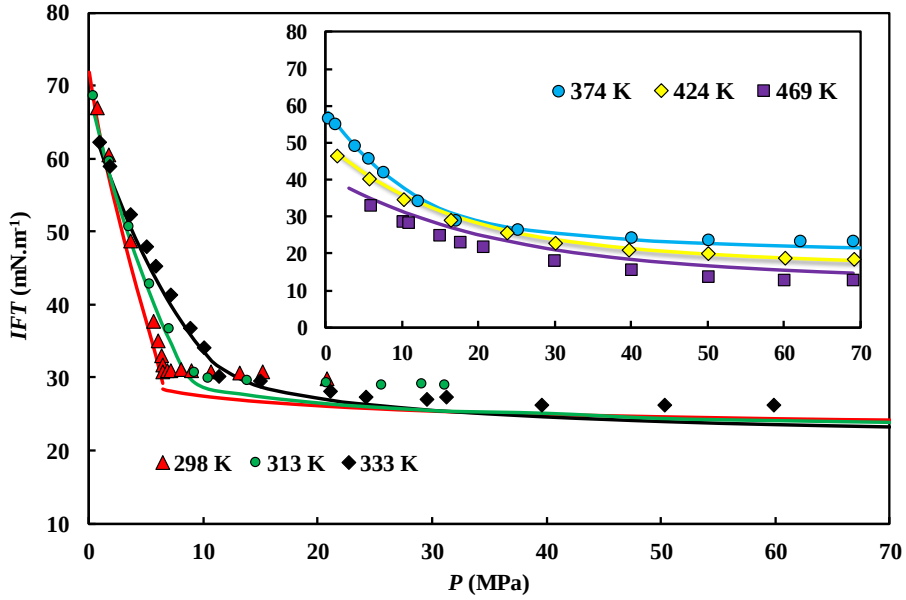

Figure 3. *IFT*−pressure diagram of CO_2 + H_2O. Symbols and solid lines represent experimental *IFT* data [10] and DGT + CPA calculations, respectively, using β_{ij} = 0.27 and constant influence parameters for CO_2 and H_2O.

As an example of the distribution of components across the interfacial region, density profiles of CO_2 and H_2O calculated for two distinct pressures at T = 298 and 373 K are shown in **Figure 4**. Observation of this figure reveals the strong adsorption of CO_2 on the CO_2-rich side of the interface, as noticed by the appearance of a peak in the CO_2 density profile, whereas H_2O density increases monotonically from the bulk CO_2-rich phase, through the interfacial region and into the H_2O-rich phase. Increasing pressure resulted in a decrease of the relative height of the CO_2 adsorption peaks, as the density of the CO_2-rich bulk phase also increased, corresponding to the isothermal phase change of CO_2 from vapour/gaseous to liquid/supercritical. These results are consistent with those of others [58–61].

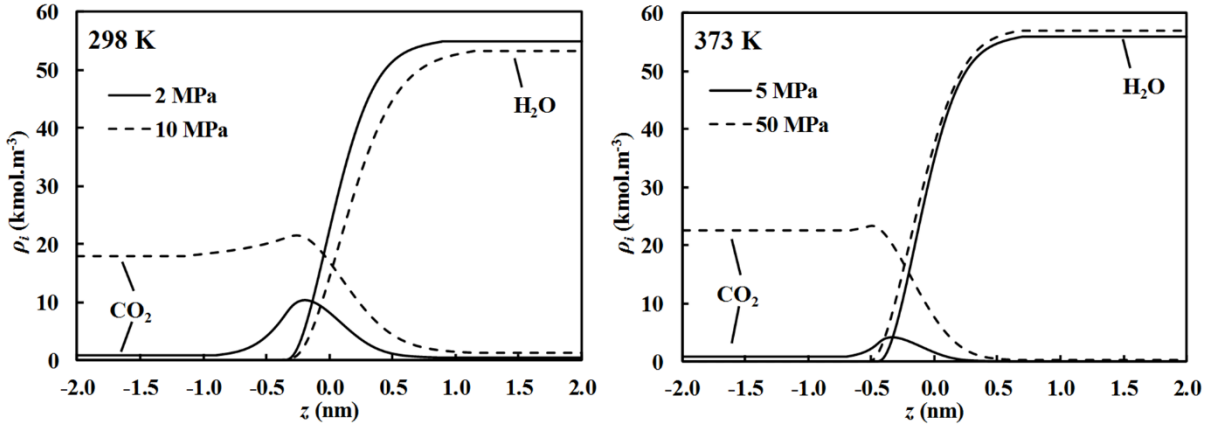

Figure 4. Density profiles across the interface as computed by the DGT + CPA approach for CO_2 + H_2O.

3.3. Predictive Modelling of the Impact of Salts

As already explained in the introduction, the increase in *IFT* upon the addition of salts appears to be related to their effect on the bulk properties as well as to the negative surface excess of ions at the interface. Based on this, we explored the idea of predicting the *IFT* between CO_2 and brines solutions by considering only the *IFT* increase associated with changes on the phase equilibria. In our approximated approach, the impact of salts on the bulk properties are modelled via the CPA EoS combined with an electrolyte model and the accompanying *IFT* predicted via the density profiles of CO_2 and H_2O through the interface in a hypothetical salt-free system computed using the DGT. In other words, the change in *IFT* is modelled by considering the salting-out effect and its influence on the energy of both bulk phases and interface in a salt-free system. Such approach does not account for the depletion of ions at the interface; however, initial results showed [33] that this method lead to successful predictions of the *IFT* of CH_4 + NaCl(aq) systems with salt molalities up to 1.91 $mol.kg^{-1}$. In this work, the model is extended to CO_2 + brine systems and the validity of such idea (approximation) is tested for higher salt molalities.

The electrolyte model used to describe the salting-out effect is based on the method proposed by Aasberg-Petersen *et al.* [70] and applicable to any EoS, where the gas solubility is modelled by adding a modified Debye-Hückel electrostatic contribution term to the fugacity coefficient term of components in the aqueous phase. For the sake of brevity, the description of the applied method for modelling the phase equilibria of CO_2 + brine mixtures along with parametrisation and evaluation procedure are provided in the Supporting Information. In short, the developed CPA EoS + Electrolyte model can be used to readily obtain an accurate description of the phase equilibria of CO_2 and brines composed of single and mixed salts, including NaCl, KCl and $CaCl_2$, for salt molalities up to 5 $mol.kg^{-1}$ and temperatures up to 473 K.

4. Results and Discussion

4.1. Experimental Measurements

The interfacial tension of CO_2 + NaCl(aq) systems were measured at temperatures ranging from 298 to 423 K and pressures up to 69.51 MPa, and salt molalities 0.98 and 1.98 $mol.kg^{-1}$. The results are listed in **Tables 4** and **5**, and plotted in **Figure 5**. It can be observed that the addition of NaCl resulted in an increase of the *IFT* from that of the CO_2 + H_2O system for all

investigated pressure and temperature conditions. This effect appeared to be less marked at T = 298 K and below the saturation pressure of CO_2, where *IFT* varies rapidly with pressure. On the other hand, measurements at higher pressures and temperatures, where *IFT* reaches a pseudo-plateau, suggest that the increment in *IFT* due to the presence of NaCl was approximately constant and nearly doubled with salt molality. Indeed, the average relative increase observed on the *IFT* values from that of the CO_2 + H_2O system [10], over the investigated pressure range, was found to amount 7.2 % (2.01 $mN.m^{-1}$) and 13.2 % (3.73 $mN.m^{-1}$) at T = 333, 373 and 423 K, and around 4.4 % (1.42 $mN.m^{-1}$) and 7.8 % (2.67 $mN.m^{-1}$) at T = 298 K, for NaCl molalities 0.98 and 1.98 $mol.kg^{-1}$, respectively, as depicted in **Figure 6**.

The measurement of any thermophysical property is always susceptible to uncertainties which affect the overall accuracy of experimental data. The combined expanded uncertainties in the interfacial tension measurements, U_c (*IFT*), were estimated as in our previous work [10]. Accordingly, U_c (*IFT*) was estimated considering the uncertainties that arise from the ADSA method, U_1 (*IFT*), and the uncertainties associated to the estimation of the density difference for the equilibrated phases, U_2 (*IFT*). The combined expanded uncertainties, estimated with a confidence greater that 95 %, for each experimental condition are given in **Tables 4** and **5**. Overall, the combined expanded uncertainty for the applied measurement method had an average value of 0.27 $mN.m^{-1}$ (0.84 %) and reached a maximum value of 0.68 $mN.m^{-1}$ (2.33 %) at the state point with the lowest calculated density difference ($\Delta\rho$ = 100.1 $kg.m^{-3}$ in **Table 4**).

Although the impact of NaCl on the *IFT* of the CO_2 + H_2O system was already studied in literature (**Table 1**), only measurements from Refs. [28,30] permit a fairly direct comparison with the values presented in this work at T = 298 K. To allow some discussion at other temperatures, data from Chalbaud *et al.* [18] at T = 373 K and different NaCl molalities are also plotted in **Figure 5** along with data from Li *et al.* [21] at T = 373 and 423 K for a brine composed of 0.864 (mole fraction) NaCl and 0.136 (mole fraction) KCl, and total salt molalities 0.98 and 1.98 $mol.kg^{-1}$. From this figure it can be observed that the data measured in this work appear to be in good agreement with those of Liu *et al.* [28], but in reasonable agreement with those of Liu *et al.* [30] and Chalbaud *et al.* [18]. CO_2 + NaCl(aq) *IFT* data from Liu *et al.* [30] at T = 298 K display a less marked change in behaviour near the saturation pressure of CO_2, with measurements showing an apparent continuous decrease of *IFT* at higher pressures. In the case of *IFT* data from Chalbaud *et al.* [18] at T = 373 K and

NaCl molalities m = 0.09 and 0.87 mol.kg^{-1}, they are generally lower than CO_2 + H_2O *IFT* at identical pressure, similar to what was already described for other experimental data sets in the introduction. Regarding the data from Li *et al.*[21], despite the discrepancies observed at T = 298 K (**Figure 1**), comparison with the isotherms at T = 373 and 423 K indicates that Na^+ and K^+ ions have similar impact on the *IFT* values as their data are very close to CO_2 + NaCl(aq) *IFT* measured in this work at identical pressure, temperature and brine molality. It is also important to note that, even though higher water salinities than those investigated in the present work can be found in deep reservoirs [11], *IFT* is expected to increase linearly with salt molality [19,21,25,31,32] and thus, the *IFT* reported here can be extrapolated to systems with higher NaCl content with fairly good confidence.

Overall, these measurements helped to resolve the inconsistencies ("low" *IFT*) observed in CO_2 + NaCl(aq) *IFT* data available in literature, while extending both pressure and temperature conditions from previous maximum (45 MPa and 398 K).

Table 4. Measured interfacial tension data of the CO_2 + H_2O + NaCl system for a salt molality 0.98 mol.kg^{-1}. The density difference used corresponds to the difference between the values estimated with the model of Duan *et al.* [40] for the CO_2-saturated brine phase and pure CO_2 obtained from REFPROP [47].

P (MPa)	$\Delta\rho$ (kg.m^{-3})	IFT (mN.m^{-1})	Experimental Error (mN.m^{-1})		
			U_1	U_2	$U_c = U_1 + U_2$
		T = 298.6 K			
3.00	980.1	53.39	0.04	0.12	0.16
4.96	918.2	42.37	0.05	0.12	0.17
5.66	882.7	38.43	0.03	0.14	0.17
10.31	236.1	32.98	0.07	0.32	0.39
15.58	177.4	32.35	0.04	0.38	0.42
20.21	145.0	32.33	0.08	0.46	0.54
		T = 333.2 K			
3.91	952.0	52.1	0.04	0.12	0.16
7.40	858.8	41.7	0.04	0.12	0.16
18.84	331.5	31.7	0.06	0.21	0.27
40.94	150.5	29.4	0.14	0.40	0.54
55.07	100.1	29.2	0.09	0.59	0.68
		T = 373.4 K			
7.19	876.9	44.04	0.06	0.11	0.17
12.32	753.1	35.94	0.11	0.11	0.22
20.14	525.2	30.60	0.05	0.13	0.18
40.89	255.9	26.81	0.05	0.21	0.26
69.50	131.6	25.10	0.06	0.38	0.44
		T = 423.3 K			
5.69	882.2	42.3	0.04	0.10	0.14
11.12	798.9	35.6	0.05	0.09	0.14
22.37	600.1	27.3	0.06	0.10	0.16
43.07	346.6	22.2	0.06	0.13	0.19
69.07	204.2	19.9	0.05	0.20	0.25

Table 5. Measured interfacial tension data of the CO_2 + H_2O + NaCl system for a salt molality 1.98 mol.kg^{-1}. The density difference used corresponds to the difference between the values estimated with the model of Duan *et al*. [40] for the CO_2-saturated brine phase and pure CO_2 obtained from REFPROP [47].

***P* (MPa)**	**$\Delta\rho$ (kg.m^{-3})**	***IFT* (mN.m^{-1})**	**Experimental Error (mN.m^{-1})**		
			U_1	U_2	$U_c = U_1 + U_2$
		***T* = 298.6 K**			
2.96	1015.9	54.98	0.04	0.12	0.16
4.12	983.3	48.43	0.03	0.12	0.15
5.69	914.7	39.59	0.03	0.14	0.17
10.25	270.4	34.09	0.06	0.29	0.35
14.82	217.1	33.74	0.07	0.33	0.40
19.90	179.8	33.61	0.07	0.39	0.46
		***T* = 333.2 K**			
4.09	981.9	53.20	0.07	0.12	0.19
7.86	875.2	42.14	0.03	0.12	0.15
18.85	363.0	33.34	0.06	0.21	0.27
41.72	178.6	31.22	0.04	0.36	0.40
54.76	132.1	30.99	0.06	0.47	0.53
		***T* = 373.3 K**			
4.61	959.3	50.69	0.08	0.11	0.19
11.49	809.5	39.01	0.13	0.11	0.24
21.94	515.3	31.76	0.08	0.14	0.22
43.18	273.1	28.31	0.11	0.21	0.32
69.51	162.6	27.16	0.04	0.34	0.38
		***T* = 423.2 K**			
5.65	918.1	44.36	0.07	0.10	0.17
12.17	815.9	36.00	0.09	0.09	0.18
21.88	642.5	29.07	0.05	0.10	0.15
44.35	369.5	23.25	0.09	0.13	0.22
69.00	236.5	21.64	0.05	0.18	0.23

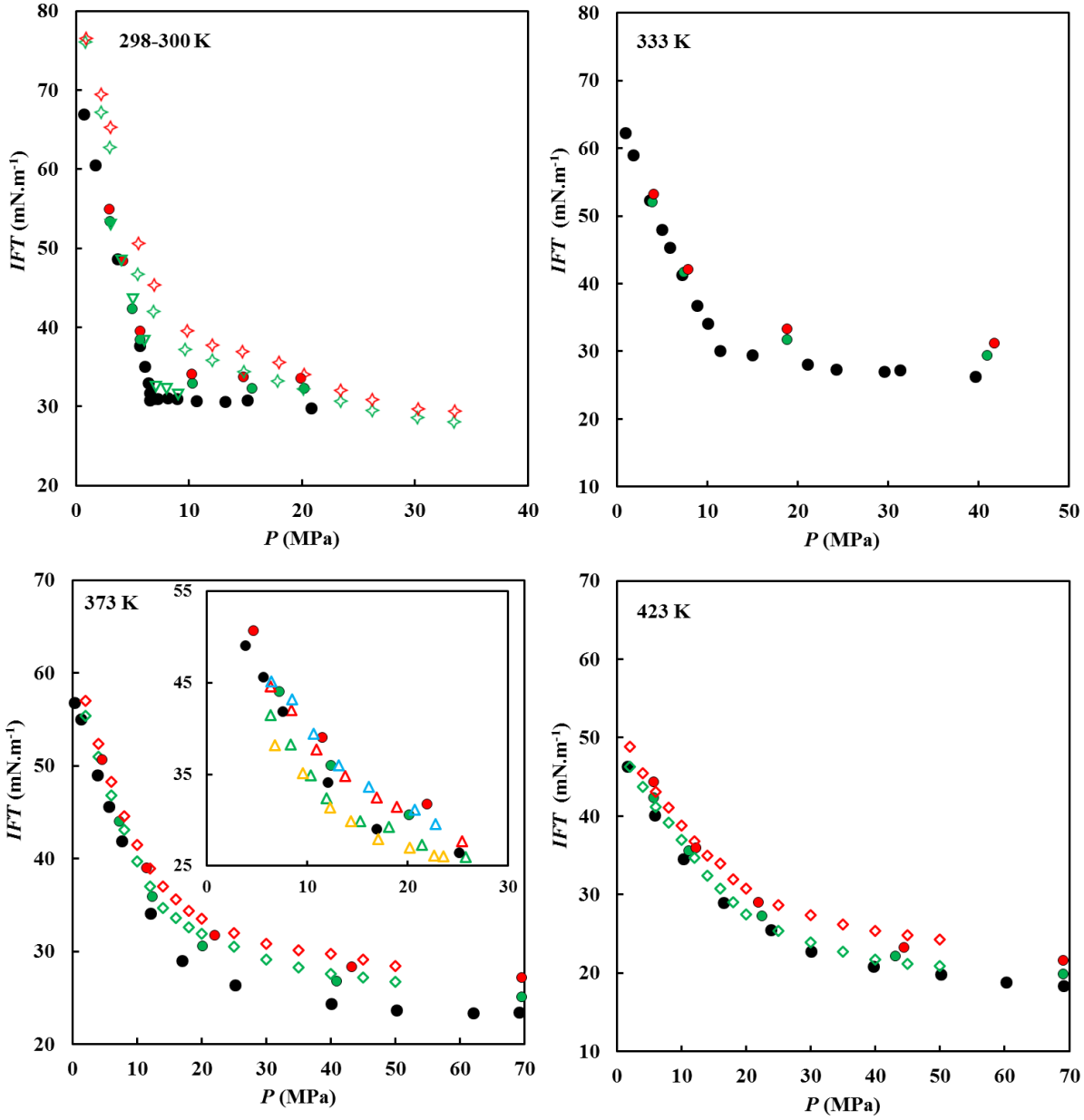

Figure 5. *IFT*−pressure diagrams of CO_2 + H_2O and CO_2 + brine systems.

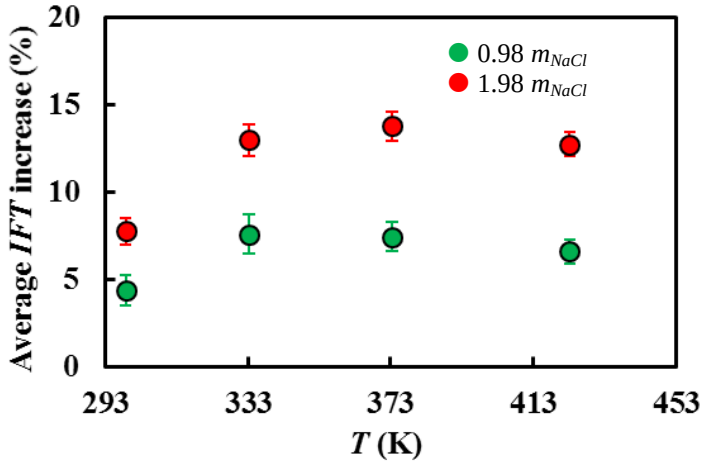

Figure 6. Average *IFT* increase−temperature diagram of CO_2 + NaCl(aq) systems. *IFT* increase was calculated relative to CO_2 + H_2O *IFT* values correlated from previous measurements [10] and averaged over the pressure range investigated. Error bars correspond to averaged experimental uncertainties listen in **Tables 4** and **5** for each isotherm.

4.2. Comparison of Model and Experiments

IFT of CO_2 + brines systems were predicted and the results compared to experimental data measured in the present work and gathered from literature for selected single and binary salt systems, as depicted in **Figures 7** and **8**. *IFT*s between CO_2 and brines have been predicted by keeping the binary interaction coefficient β_{ij} = 0.27 between CO_2 and H_2O within the DGT framework and the phase equilibria modelled trough the CPA EoS + Electrolyte model, without any further adjustments to *IFT* data.

As shown in **Figures 7** and **8**, the present modelling approach can adequately predict the increase in *IFT* due to the presence of salts such as NaCl, KCl and $CaCl_2$ as well as their mixtures; very good agreement with experimental data measured here for CO_2 + NaCl(aq) at T = 333 and 373 K and salt molalities up to 1.98 mol.kg^{-1} is observed. In addition, as substantiated experimentally [19,21,25,31,32], predicted *IFT* values increase linearly with salt molalities; as an example, results for CO_2 + [0.864 NaCl + 0.136 KCl](aq) at T = 373 K and selected isobars are plotted in **Figure 9.** However, for very concentrated brines, and depending on the computed CO_2 + H_2O *IFT* for the examined isotherm, the model appears to overpredict severely the *IFT* of CO_2 + brine systems, in particular for brines containing $CaCl_2$. It is important to mention that *IFT* data measured by Aggelopoulos *et al.*[31,32] for diluted brines containing $CaCl_2$ persisted in being lower than CO_2 + H_2O *IFT* data [10], as shown in **Figures** 7**b** and **8b**, similar to what was already described for other data sets (**Figure 1**); yet, the differences between predicted and experimentally determined *IFT* values

at higher salt concentrations cannot be attributed to the inconsistencies in the experiments alone. In turn, such overprediction of *IFT* values may be most probably due to the strong salting-out effect of $CaCl_2$ compared to NaCl or KCl, which is intrinsically related to the ionic strength of the brine. Based on these observations and on the modelling results for the examined brines, it can be argued that such approximated treatment of the rise in *IFT* due the presence of salts (via solubility change) appears to be adequate only for brines with low and medium ionic strength (up to I = 2.7 mol.kg^{-1} or 0.9 m_{CaCl_2}) under the temperature and pressure conditions examined.

The modelling results explained above are better interpreted by means of the Gibbs adsorption equation. Accordingly, the change in CO_2 + brine *IFT* ($d\gamma$) can be related to the chemical potentials (μ) of CO_2 and ions as follows [71]:

$$-d\gamma = \Gamma_{CO_2}\mu_{CO_2} + \Gamma_{cation}\mu_{cation} + \Gamma_{anion}\mu_{anion} \qquad \text{at constant } T \qquad \textbf{(8)}$$

where Γ_i is the surface/interfacial excess (or adsorption/desorption) of species *i*. By convention, a dividing surface is chosen such that Γ_{H_2O} = 0. From this equation it can be shown that changes on CO_2 + brine *IFT* are related to the individual contribution of each species in the system: increasing the chemical potential of a species with positive surface excess (such as CO_2) would result in a decrease in *IFT*, whereas increasing the chemical potential of a species with negative surface excess (such as the salt ions examined) would result in an increase in *IFT*. Therefore, it can be concluded that the differences between predictions and experimental *IFT* data for CO_2 + brines may be due to the fact that in the model only the salting-out effects were accounted for (*i.e.*, decrease in the chemical potential of CO_2) while the contribution of ions to the *IFT* has been neglected. Nevertheless, the modelling results obtained here are encouraging, given the fully predictive treatment of the current approach when compared to that often used based on purely empirical methods [18,21,25,72–74].

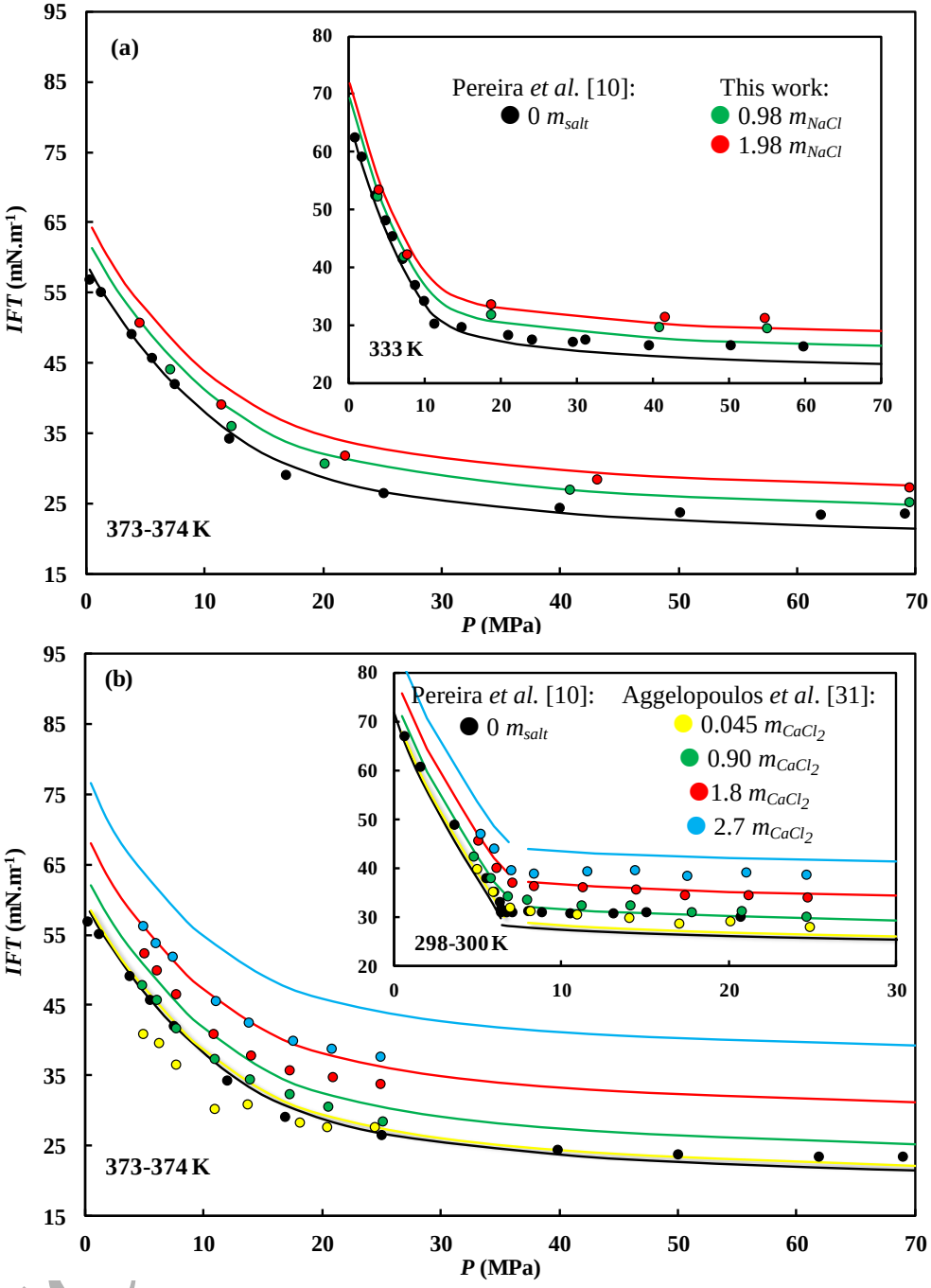

Figure 7. *IFT*−pressure diagrams of **(a)** CO_2 + NaCl(aq) and **(b)** CO_2 + $CaCl_2$(aq) systems. Solid lines represent DGT predictions at pertinent salt molalities and temperatures. Predictions were obtained using a binary interaction coefficient β_{ij} = 0.27, as estimated for the CO_2 + H_2O system.

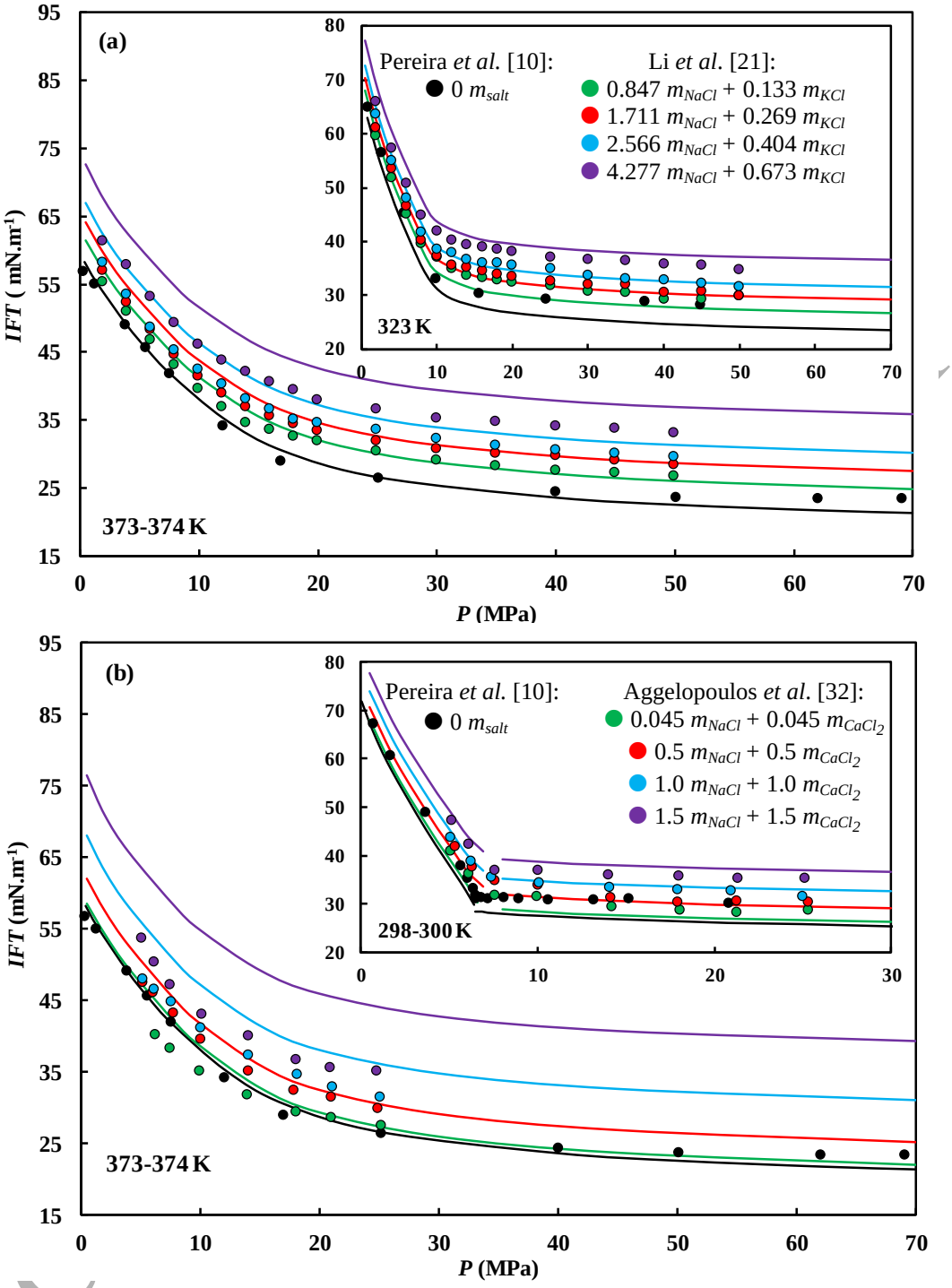

Figure 8. *IFT*−pressure diagrams of **(a)** CO_2 + [NaCl + KCl](aq) and **(b)** CO_2 + [NaCl + $CaCl_2$](aq) systems. Solid lines represent DGT predictions at pertinent salt molalities and temperatures. Predictions were obtained using a binary interaction coefficient β_{ij} = 0.27, as estimated for the CO_2 + H_2O system.

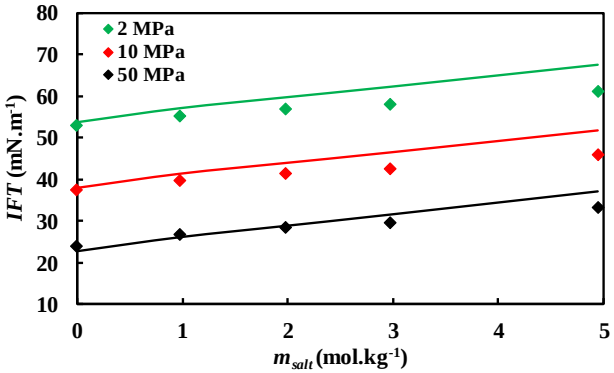

Figure 9. *IFT*−total salt molality diagram of CO_2 + [0.864 NaCl + 0.136 KCl](aq) systems at T = 373 K. Symbols represent experimental data from Li *et al.* [21] for fixed pressure. *IFT* data points for zero salt molality were interpolated from CO_2 + H_2O *IFT* data [10]. Solid lines represent DGT predictions.

5. Conclusions

In this communication we have investigated experimentally and theoretically the interfacial tension between CO_2 and brines over a broad range of conditions, including those relevant to geological storage of CO_2 in deep aquifers. *IFT*s were measured for CO_2 + NaCl(aq) systems from ambient conditions up to 423 K and 69.51 MPa, and for two salt molalities, 0.98 and 1.98 mol.kg^{-1}. Additionally, a modelling approach for predicting the impact of salts on the magnitude of the interfacial tension of gas + brine systems, established in a previous work [33], was further extended to CO_2 + brine systems and tested for higher salt molalities. The applied modelling approach consisted on accounting for the salting-out effect on the solubility of the gas, via the CPA EoS in combination with an electrolyte model, and subsequent computation of density profiles and accompanied *IFT* in a hypothetical salt-free system with the DGT.

Experimental results clearly showed that CO_2 + NaCl(aq) *IFT* exceeded that of the corresponding salt-free system for all pressure and temperature states examined. This served to amplify previous studies and to resolve some of the inconsistencies observed for data reported in literature, in particular at low temperatures where various studies reported *IFT* values lower than that of CO_2 + H_2O. The increase in interfacial tension from the salt-free system averaged an amount between 1.42 and 2.01 mN.m^{-1} for m_{NaCl} = 0.98 mol.kg^{-1} and between 2.67 and 3.73 mN.m^{-1} for m_{NaCl} = 1.98 mol.kg^{-1}. This corresponds to an average relative increase from CO_2 + H_2O *IFT* between 4.4 and 13.2%, over the examined range of pressures, temperatures and salt molalities.

IFT data of CO_2 + brine systems, including single and binary salt mixtures of NaCl, $CaCl_2$ and KCl, measured in this work and gathered from literate were used to assess the predictive capabilities of the modelling scheme. The only adjusted parameter, the binary coefficient for the cross influence parameter between CO_2 and H_2O within the framework of the DGT, was estimated from one interfacial tension data point of CO_2 + H_2O at intermediate conditions. Comparison with experiments showed that the model is able to predict, with a high degree of accuracy, CO_2 + brine interfacial tensions for brine solutions of low and medium ionic strength (up to I = 2.7 mol.kg^{-1}). The dependence of *IFT* on salt molality and the additive effects of different salts are also effectively predicted, although the *IFT* is overpredicted for concentrated brines solutions with the current model. All things considered, we have demonstrated that the model developed in this work is a useful tool for predicting interfacial tensions relevant to CO_2 storage in deep saline aquifers as function of pressure, temperature and brine composition.

6. Acknowledgements

This research work is part of an ongoing Joint Industrial Project (JIP) conducted jointly at the Institute of Petroleum Engineering, Heriot-Watt University and the CTP laboratory of MINES ParisTech. The JIPs is supported by Chevron, GALP Energia, Linde AG Engineering Division, OMV, Petroleum Expert, Statoil, TOTAL and National Grid Carbon Ltd, which is gratefully acknowledged. The participation of National Grid Carbon in the JIP was funded by the European Commission's European Energy Programme for Recovery. The authors would also like to thank the members of the steering committee for their fruitful comments and discussions. Luís M. C. Pereira acknowledges the financial support from Galp Energia through his PhD grant.

7. References

[1] B. Smit, *Carbon Capture and Storage: introductory lecture*, Faraday Discuss. **192**, 9–25 (2016).

[2] S. Bachu, *Sequestration of CO_2 in geological media: criteria and approach for site selection in response to climate change*, Energy Convers. Manag. **41**, 953–970 (2000).

[3] Z. Li, M. Dong, S. Li, S. Huang, *CO_2 sequestration in depleted oil and gas reservoirs—caprock characterization and storage capacity*, Energy Convers. Manag. **47**, 1372–1382 (2006).

[4] K. Michael, A. Golab, V. Shulakova, J. Ennis-King, G. Allinson, S. Sharma, T. Aiken, *Geological storage of CO_2 in saline aquifers-A review of the experience from existing storage operations*, Int. J. Greenh. Gas Control. **4**, 659–667 (2010).

[5] IPCC, *Special Report on Carbon Dioxide Capture and Storage*, Cambridge University Press (2005).

[6] P. Chiquet, J.-L. Daridon, D. Broseta, S. Thibeau, *CO_2/water interfacial tensions under pressure and temperature conditions of CO_2 geological storage*, Energy Convers. Manag. **48**, 736–744 (2007).

[7] V. Shah, D. Broseta, G. Mouronval, F. Montel, *Water/acid gas interfacial tensions and their impact on acid gas geological storage*, Int. J. Greenh. Gas Control. **2**, 594–604 (2008).

[8] S. Iglauer, C.H. Pentland, A. Busch, *CO_2 wettability of seal and reservoir rocks and the implications for carbon geo-sequestration*, Water Resour. Res. **51**, 729–774 (2015).

[9] G. Pijaudier-Cabot, J.-M. Pereira, *Geomechanics in CO_2 Storage Facilities*, John Wiley & Sons, Inc. (2013).

[10] L.M.C. Pereira, A. Chapoy, R. Burgass, M.B. Oliveira, J.A.P. Coutinho, B. Tohidi, *Study of the impact of high temperatures and pressures on the equilibrium densities and interfacial tension of the carbon dioxide/water system*, J. Chem. Thermodyn. **93**, 404–415 (2016).

[11] S. Bachu, D.B. Bennion, *Interfacial tension between CO_2 , freshwater, and brine in the range of pressure from (2 to 27) MPa, temperature from (20 to 125) °C, and water salinity from (0 to 334 000) mg·L $^{-1}$*, J. Chem. Eng. Data. **54**, 765–775 (2009).

[12] J. Ralston, T.W. Healy, *Specific cation effects on water structure at the air-water and air-octadecanol monolayer-water interfaces*, J. Colloid Interface Sci. **42**, 629–644 (1973).

[13] K. Johansson, J.C. Eriksson, *Γ and $d\gamma/dT$ measurements on aqueous solutions of 1,1-electrolytes*, J. Colloid Interface Sci. **49**, 469–480 (1974).

[14] P.K. Weissenborn, R.J. Pugh, *Surface tension of aqueous solutions of electrolytes: relationship with ion hydration, oxygen solubility, and bubble coalescence*, J. Colloid Interface Sci. **184**, 550–563 (1996).

[15] L.M. Pegram, M.T. Record, *Hofmeister salt effects on surface tension arise from partitioning of anions and cations between bulk water and the air−water interface*, J. Phys. Chem. B. **111**, 5411–5417 (2007).

[16] Y. Levin, A.P. dos Santos, A. Diehl, *Ions at the air-water interface: An end to a hundred-year-old mystery?*, Phys. Rev. Lett. **103**, 257802 (2009).

[17] Y. Marcus, *Effect of ions on the structure of water: structure making and breaking.*, Chem. Rev. **109**, 1346–70 (2009).

[18] C. Chalbaud, M. Robin, J.-M. Lombard, F. Martin, P. Egermann, H. Bertin, *Interfacial tension measurements and wettability evaluation for geological CO_2 storage*, Adv. Water Resour. **32**, 98–109 (2009).

[19] C. Duchateau, D. Broseta, *A simple method for determining brine–gas interfacial tensions*, Adv. Water Resour. **42**, 30–36 (2012).

[20] M.J. Hey, D.W. Shield, J.M. Speight, M.C. Will, *Surface tensions of aqueous solutions of some 1:1 electrolytes*, J. Chem. Soc. Faraday Trans. 1 Phys. Chem. Condens. Phases. **77**, 123 (1981).

[21] X. Li, E. Boek, G.C. Maitland, J.P.M. Trusler, *Interfacial tension of (brines + CO_2): (0.864 NaCl + 0.136 KCl) at yemperatures between (298 and 448) K, pressures between (2 and 50) MPa, and total molalities of (1 to 5) mol·kg $^{-1}$*, J. Chem. Eng. Data. **57**, 1078–1088 (2012).

[22] M.J. Argaud, *Predicting the interfacial tension of brine/gas (or condensates) systems*, in: 3rd Eur. Core Anal. Symp., Society of Core Analysts (1992).

[23] X. Li, D.A. Ross, J.P.M. Trusler, G.C. Maitland, E.S. Boek, *Molecular dynamics simulations of CO_2 and brine interfacial tension at high temperatures and pressures.*, J. Phys. Chem. B. **117**, 5647–52 (2013).

[24] V.S. Patwardhan, A. Kumar, *A unified approach for prediction of thermodynamic properties of aqueous mixed-electrolyte solutions. Part II: Volume, thermal, and other properties*, AIChE J. **32**, 1429–1438 (1986).

[25] X. Li, E.S. Boek, G.C. Maitland, J.P.M. Trusler, *Interfacial tension of (brines + CO_2): $CaCl_2$ (aq), $MgCl_2$ (aq), and $NaCl_2SO_4$ (aq) at temperatures between (343 and 423) K, pressures between (2 and 50) MPa, and molalities of (0.5 to 5) mol/kg*, J. Chem. Eng. Data. **57**, 1369–1375 (2012).

[26] A. Georgiadis, G. Maitland, J.P.M. Trusler, A. Bismarck, *Interfacial tension measurements of the (H_2O + CO_2) system at elevated pressures and temperatures*, J. Chem. Eng. Data. **55**, 4168–4175 (2010).

[27] R. Massoudi, A.D. King, *Effect of pressure on the surface tension of aqueous solutions. Adsorption of hydrocarbon gases, carbon dioxide, and nitrous oxide on aqueous solutions of sodium chloride and tetrabutylammonium bromide at 25 ^{o}C.*, J. Phys. Chem. **79**, 1670–1675 (1975).

[28] Y. Liu, M. Mutailipu, L. Jiang, J. Zhao, Y. Song, L. Chen, *Interfacial tension and contact angle measurements for the evaluation of CO_2-brine two-phase flow characteristics in porous media*, Environ. Prog. Sustain. Energy. **34**, 1756–1762

(2015).

[29] M. Arif, A.Z. Al-Yaseri, A. Barifcani, M. Lebedev, S. Iglauer, *Impact of pressure and temperature on CO_2-brine-mica contact angles and CO_2-brine interfacial tension: Implications for carbon geo-sequestration*, J. Colloid Interface Sci. **462**, 208–215 (2016).

[30] Y. Liu, H.A. Li, R. Okuno, *Measurements and Modeling of Interfacial Tension for CO_2/CH_4/Brine Systems under Reservoir Conditions*, Ind. Eng. Chem. Res. **55**, 12358–12375 (2016).

[31] C.A. Aggelopoulos, M. Robin, E. Perfetti, O. Vizika, *CO_2/$CaCl_2$ solution interfacial tensions under CO_2 geological storage conditions: Influence of cation valence on interfacial tension*, Adv. Water Resour. **33**, 691–697 (2010).

[32] C.A. Aggelopoulos, M. Robin, O. Vizika, *Interfacial tension between CO_2 and brine ($NaCl+CaCl_2$) at elevated pressures and temperatures: The additive effect of different salts*, Adv. Water Resour. **34**, 505–511 (2011).

[33] K. Kashefi, L.M.C. Pereira, A. Chapoy, R. Burgass, B. Tohidi, *Measurement and modelling of interfacial tension in methane/water and methane/brine systems at reservoir conditions*, Fluid Phase Equilib. **409**, 301–311 (2016).

[34] J.W. Cahn, J.E. Hilliard, *Free Energy of a Nonuniform System. I. Interfacial Free Energy*, J. Chem. Phys. **28**, 258 (1958).

[35] P. Cheng, D. Li, L. Boruvka, Y. Rotenberg, A.W. Neumann, *Automation of axisymmetric drop shape analysis for measurements of interfacial tensions and contact angles*, Colloids and Surfaces. **43**, 151–167 (1990).

[36] B. Song, J. Springer, *Determination of interfacial tension from the profile of a pendant drop using computer-aided image processing: 2. Experimental*, J. Colloid Interface Sci. **184**, 77–91 (1996).

[37] M. Hoorfar, a W Neumann, *Recent progress in axisymmetric drop shape analysis (ADSA).*, Adv. Colloid Interface Sci. **121**, 25–49 (2006).

[38] A.W. Neumann, R. David, Y. Zuo, *Applied surface thermodynamics*, Second ed., CRC Press Taylor & Francis Group (2010).

[39] W. Yan, S. Huang, E.H. Stenby, *Measurement and modeling of CO_2 solubility in NaCl brine and CO_2–saturated NaCl brine density*, Int. J. Greenh. Gas Control. **5**, 1460–1477 (2011).

[40] Z. Duan, J. Hu, D. Li, S. Mao, *Densities of the CO_2 –H_2O and CO_2 –H_2O–NaCl systems up to 647 K and 100 MPa*, Energy & Fuels. **22**, 1666–1674 (2008).

[41] Z. Duan, N. Møller, J.H. Weare, *An equation of state for the CH_4-CO_2-H_2O system: I. Pure systems from 0 to 1000°C and 0 to 8000 bar*, Geochim. Cosmochim. Acta. **56**, 2605–2617 (1992).

[42] Z. Duan, R. Sun, *An improved model calculating CO_2 solubility in pure water and aqueous NaCl solutions from 273 to 533 K and from 0 to 2000 bar*, Chem. Geol. **193**, 257–271 (2003).

[43] Z. Duan, R. Sun, C. Zhu, I.-M. Chou, *An improved model for the calculation of CO_2 solubility in aqueous solutions containing Na^+, K^+, Ca^{2+}, Mg^{2+}, Cl^-, and SO_4^{2-}*, Mar. Chem. **98**, 131–139 (2006).

[44] J.C. Peiper, K.S. Pitzer, *Thermodynamics of aqueous carbonate solutions including mixtures of sodium carbonate, bicarbonate, and chloride*, J. Chem. Thermodyn. **14**, 613–638 (1982).

[45] E.C. Efika, R. Hoballah, X. Li, E.F. May, M. Nania, Y. Sanchez-Vicente, J.P. Martin Trusler, *Saturated phase densities of (CO_2 + H_2O) at temperatures from (293 to 450) K and pressures up to 64 MPa*, J. Chem. Thermodyn. **93**, 347–359 (2016).

[46] C.E. Deering, E.C. Cairns, J.D. McIsaac, A.S. Read, R. a. Marriott, *The partial molar volumes for water dissolved in high-pressure carbon dioxide from T=(318.28 to 369.40)K and pressures to p=35MPa*, J. Chem. Thermodyn. **93**, 337–346 (2016).

[47] E.W. Lemmon, M.L. Huber, M.O. McLinden, *NIST Reference Fluid Thermodynamic and Transport Properties — REFPROP, Version 9.0, NIST, Gaithersburg, MD*, (2010).

[48] J.D. van der Waals, *Thermodynamische Theorie der Kapillarität unter Voraussetzung stetiger Dichteänderung*, Z. Phys. Chem. **13**, 657–725 (1894).

[49] H.T. Davis, *Statistical mechanics of phases, interfaces and thin films*, Wiley (1995).

[50] B.F. McCoy, H.T. Davis, *Free-energy theory of inhomogeneous fluids*, Phys. Rev. A. **20**, 1201–1207 (1979).

[51] B.S. Carey, L.E. Scriven, H.T. Davis, *Semiempirical theory of surface tension of binary systems*, AIChE J. **26**, 705–711 (1980).

[52] P.M.W. Cornelisse, *The square gradient theory applied: Simultaneous modelling of interfacial tension and phase behaviour* (PhD thesis), Delft University of Technology, The Netherlands, (1997).

[53] L.M.C. Pereira, *Interfacial Tension of Reservoir Fluids: an Integrated Experimental and Modelling Investigation* (PhD thesis), Heriot-Watt University, UK, (2016).

[54] V. Bongiorno, H.T. Davis, *Modified Van der Waals theory of fluid interfaces*, Phys. Rev. A. **12**, 2213–2224 (1975).

[55] V. Bongiorno, L.E. Scriven, H.T. Davis, *Molecular theory of fluid interfaces*, J. Colloid Interface Sci. **57**, 462–475 (1976).

[56] B.S. Carey, *The gradient theory of fluid interfaces* (PhD thesis), University of Minnesota, USA, (1979).

[57] L.M.C. Pereira, A. Chapoy, R. Burgass, B. Tohidi, *Measurement and modelling of high pressure density and interfacial tension of (gas+n-alkane) binary mixtures*, J. Chem. Thermodyn. **97**, 55–69 (2016).

[58] T. Lafitte, B. Mendiboure, M.M. Piñeiro, D. Bessières, C. Miqueu, *Interfacial properties of water/CO_2: a comprehensive description through a Gradient Theory-SAFT-VR Mie approach.*, J. Phys. Chem. B. **114**, 11110–6 (2010).

[59] G. Niño-Amézquita, D. van Putten, S. Enders, *Phase equilibrium and interfacial properties of water+CO_2 mixtures*, Fluid Phase Equilib. **332**, 40–47 (2012).

[60] X.-S. Li, J.-M. Liu, D. Fu, *Investigation of interfacial tensions for carbon dioxide aqueous solutions by perturbed-chain statistical associating fluid theory combined with density-gradient theory*, Ind. Eng. Chem. Res. **47**, 8911–8917 (2008).

[61] J.M. Míguez, J.M. Garrido, F.J. Blas, H. Segura, A. Mejía, M.M. Piñeiro, *Comprehensive characterization of interfacial behavior for the mixture CO_2 + H_2O + CH_4 : Comparison between atomistic and coarse grained molecular simulation models and density gradient theory*, J. Phys. Chem. C. **118**, 24504–24519 (2014).

[62] S. Khosharay, F. Varaminian, *Experimental and modeling investigation on surface tension and surface properties of (CH4 + H2O), (C2H6 + H2O), (CO2 + H2O) and (C3H8 + H2O) from 284.15 K to 312.15 K and pressures up to 60 bar*, Int. J. Refrig. **47**, 26–35 (2014).

[63] S. Khosharay, M. Abolala, F. Varaminian, *Modeling the surface tension and surface properties of (CO_2 + H_2O) and (H_2S + H_2O) with gradient theory in combination with sPC–SAFT EOS and a new proposed influence parameter*, J. Mol. Liq. **198**, 292–298 (2014).

[64] Y.T.F. Chow, D.K. Eriksen, A. Galindo, A.J. Haslam, G. Jackson, G.C. Maitland, J.P.M. Trusler, *Interfacial tensions of systems comprising water, carbon dioxide and diluent gases at high pressures: Experimental measurements and modelling with SAFT-VR Mie and square-gradient theory*, Fluid Phase Equilib. **407**, 159–176 (2016).

[65] G.M. Kontogeorgis, M.L. Michelsen, G.K. Folas, S. Derawi, N. von Solms, E.H. Stenby, *Ten years with the CPA (cubic-plus-association) equation of state. Part 1. Pure compounds and self-associating systems*, Ind. Eng. Chem. Res. **45**, 4855–4868 (2006).

[66] G.M. Kontogeorgis, M.L. Michelsen, G.K. Folas, S. Derawi, N. von Solms, E.H. Stenby, *Ten years with the CPA (cubic-plus-association) equation of state. Part 2. Cross-associating and multicomponent systems*, Ind. Eng. Chem. Res. **45**, 4869–4878 (2006).

[67] A.J. Queimada, C. Miqueu, I.M. Marrucho, G.M. Kontogeorgis, J.A.P. Coutinho, *Modeling vapor–liquid interfaces with the gradient theory in combination with the CPA equation of state*, Fluid Phase Equilib. **228**–**229**, 479–485 (2005).

[68] G.M. Kontogeorgis, I. V Yakoumis, H. Meijer, E. Hendriks, T. Moorwood, *Multicomponent phase equilibrium calculations for water-methanol-alkane mixtures*, Fluid Phase Equilib. **158**–**160**, 201–209 (1999).

[69] I. Tsivintzelis, G.M. Kontogeorgis, M.L. Michelsen, E.H. Stenby, *Modeling phase equilibria for acid gas mixtures using the CPA equation of state. Part II: Binary mixtures with CO_2*, Fluid Phase Equilib. **306**, 38–56 (2011).

[70] K. Aasberg-Petersen, E. Stenby, A. Fredenslund, *Prediction of high-pressure gas solubilities in aqueous mixtures of electrolytes*, Ind. Eng. Chem. Res. **30**, 2180–2185 (1991).

[71] C.J. Radke, *Gibbs adsorption equation for planar fluid-fluid interfaces: Invariant formalism.*, Adv. Colloid Interface Sci. **222**, 600–14 (2015).

[72] D.B. Bennion, S. Bachu, *Correlations for the Interfacial Tension Between Supercritical Phase CO_2 and Equilibrium Brines at In Situ Conditions*, in: SPE Annu. Tech. Conf. Exhib., Society of Petroleum Engineers (2008).

[73] R.P. Sutton, *An improved model for water-hydrocarbon surface tension at reservoir conditions*, in: SPE Annu. Tech. Conf. Exhib., Society of Petroleum Engineers (2009).

[74] Z. Li, S. Wang, S. Li, W. Liu, B. Li, Q.-C. Lv, *Accurate Determination of the CO_2–Brine Interfacial Tension Using Graphical Alternating Conditional Expectation*, Energy & Fuels. **28**, 624–635 (2014).